Snow Melt Onset Over Arctic Sea Ice from SMMR and SSM/I-SSMIS Brightness Temperatures, Version 5

USER GUIDE

How to Cite These Data

As a condition of using these data, you must include a citation:

Bliss, A. C., M. Anderson, and S. Drobot. 2022. *Snow Melt Onset Over Arctic Sea Ice from SMMR and SSM/I-SSMIS Brightness Temperatures, Version 5*. [Indicate subset used]. Boulder, Colorado USA. NASA National Snow and Ice Data Center Distributed Active Archive Center. https://doi.org/10.5067/TRGWQ0ONTQG5. [Date Accessed].

FOR QUESTIONS ABOUT THESE DATA, CONTACT NSIDC@NSIDC.ORG

FOR CURRENT INFORMATION, VISIT https://nsidc.org/data/NSIDC-0105

National Snow and Ice Data Center

TABLE OF CONTENTS

1 DATA DESCRIPTION

1.1 Parameters

The main parameter for this data set is Snow Melt Onset Date (SMOD) over Arctic sea ice, where its value represents the Day of Year (DOY) when microwave brightness temperatures increases sharply due to the presence of liquid water in the snowpack. This data set also includes statistical analyses of each grid cell's SMOD over the period between 1979 through 2022. Table 1 includes summary of the flag values and their respective meanings as a SMOD variable and statistical variable reports within the netCDF (.nc) file.

Table 1. Summary of flag meanings as a SMOD variable and statistics variable.

Flag Value	Meaning	
	Description	**Statistics**
-150	Open water or missing melt date; no data	
-100	Pole hole; no melt dates were calculated	
-50	Land mask; no melt dates were calculated	
-255	Sea ice did not melt	N/A

1.2 File Information

1.2.1 Format

Data are provided in netCDF (.nc) file format.

PNG (.png) browse images and Extensible Markup Language (.xml) files with associated metadata are also provided.

1.2.2 File Contents

NetCDF file contents are described in Table 2.

Table 2. Description of netCDF Variables

Variable Name	Description	Units
SMOD	Annual snow melt onset date	Day of Year (DOY); see Table 1 for more details
mean	Mean snow melt onset date	DOY
median	Median snow melt onset date	DOY
latest	Latest (maximum) snow melt onset date	DOY
earliest	Earliest (minimum) snow melt onset date	DOY
range	Latest minus earliest snow melt onset date	Days
stdev	Standard deviation of snow melt onset dates	Days
trend	Decadal trend in snow melt onset based on a least squares linear regression	Days per Decade
latitude	Latitude	Degrees North
longitude	Longitude	Degrees East
projection	Description of projected coordinate system	N/A
time	Time	Days since 1970-01-01
x	Projected x coordinate	Meters
y	Projected y coordinate	Meters

One browse image is provided for each year of data showing the annual SMOD; Figure 1 contains a sample image. One browse image is also provided for each statistical field, as exemplified by Figure 2.

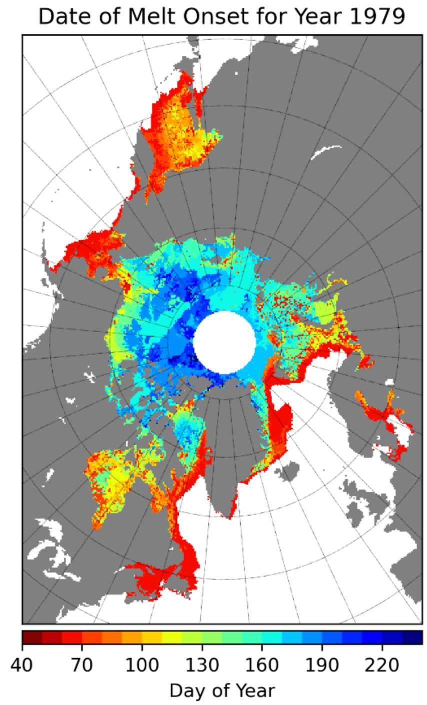

Figure 1. Sample browse image showing snow melt onset dates for 1979.

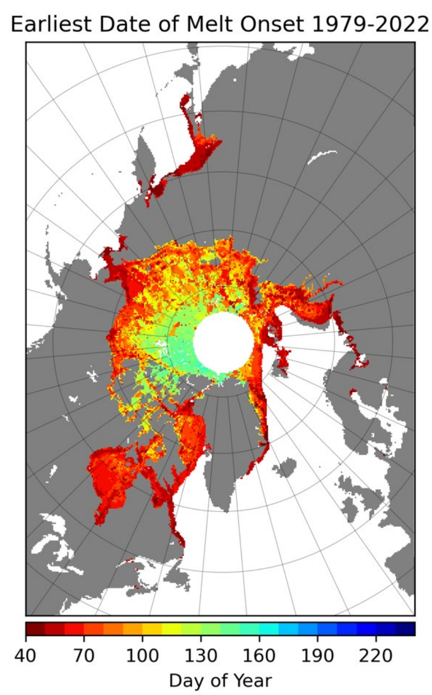

Figure 2. Sample statistical-field browse image showing the earliest snowmelt onset date recorded between 1979 and 2022.

1.2.3 Directory Structure

Data are available for download via HTTPS; the link is accessible under the heading listed as "Data Access & Tools" on the data set landing page. Within the file directory, the browse images function is available in the subfolder labeled "Browse".

1.2.4 Naming Convention

The netCDF file name is:

`SMOD_1979-2022_v05r00.nc`

Browse images showing the annual snow melt onset date are named according to the following convention and as described in Table 3:

`melt_<year>_v05r00_n.png`

Table 3. Snow Melt Onset Date Browse Images

Variable	Description
melt	Indicates the file is part of the Snow Melt Onset Over Arctic Sea Ice from SMMR and SSM/I-SSMIS Brightness Temperatures data set
<year>	Year of data represented by the image
v05	Data set version number (e.g. 05)
r00	Data set revision number (e.g. 00)
n	Hemisphere (n = Northern)

Browse images for statistical fields are named according to the following convention and as described in Table 4:

`melt_<field>_1979-2022_v05r00_n.png`

Table 4. Statistical Browse Images

Variable	Description
melt	Indicates the file is part of the Snow Melt Onset Over Arctic Sea Ice from SMMR and SSM/I-SSMIS Brightness Temperatures data set
<field>	Statistical field represented in the image (e.g. range, earliest, latest)
1979-2022	Data set temporal coverage
v05	Data set version number (e.g. 05)
r00	Data set revision number (e.g. 00)
N	Hemisphere (n = Northern)

1.3 Spatial Information

1.3.1 Coverage

Data cover the Northern Hemisphere, except for three circular gaps centered over the pole that correspond to the three satellite records. Data from the SMMR period (1978 to 1987) have a gap with a radius of 611 km, located poleward of 84.5 degrees North. Data from the SSM/I period (1987 through 2007) have a polar gap with a radius of 311 km, located poleward of 87.2 degrees North. Lastly, data from the SSMIS period (2008 through 2022) have a gap poleward of 89.2° North. See the Polar Stereographic Projection and Grid spatial coverage map for details.

1.3.2 Resolution

Resolution is available at 25 km, centering around the northern polar region.

1.3.3 Geolocation

Information for geolocating this data set on the 25 km Northern Hemisphere Polar Stereographic Grids are described in Table 5 and Table 6. For more information, see the Polar Stereographic Projections and Grid web page.

Table 5. Geolocation Details

Geographic coordinate system	Unspecified datum based upon the Hughes 1980 ellipsoid
Projected coordinate system	NSIDC Sea Ice Polar Stereographic North
Longitude of true origin	-45
Latitude of true origin	70
Scale factor at longitude of true origin	1
Datum	Not_specified_based_on_Hughes_1980_ellipsoid
Ellipsoid/spheroid	Hughes 1980
Units	meters
False easting	0
False northing	0
EPSG code	3411
PROJ4 string	`+proj=stere +lat_0=90 +lat_ts=70 +lon_0=-45 +x_0=0 +y_0=0 +a=6378273 +b=6356889.449 +units=m +no_defs +type=crs`
Reference	https://epsg.io/3411

Table 6. Grid Details

Grid cell size (x, y pixel dimensions)	25.0 km
Number of rows	448
Number of columns	304
Geolocated lower left point in grid	33.92° N, 279.26° W
Nominal gridded resolution	25 km x 25 km
Grid rotation	N/A
ulxmap – x-axis map coordinate of the center of the upper-left pixel (XLLCORNER for ASCII data)	-3850 projected km
ulymap – y-axis map coordinate of the center of the upper-left pixel (YLLCORNER for ASCII data)	5850 projected km

1.4 Temporal Information

1.4.1 Coverage

This data set extends from 1979 through 2022. While the entire time series has been reprocessed, snow melt onset dates were derived from brightness temperatures acquired from multiple platforms, as described in Table 7. In this newest version, the algorithm has been updated to use a variable DOY start date; start date is now defined as the first day following the day of the annual maximum sea ice extent (SIE).

Table 7. Temporal Coverage by Input Sensor

Platform / Sensor	Start Date	End Date
Nimbus-7 SMMR	01 January 1979	20 August 1987[1]
DMSP F8 SSM/I	01 January 1988	18 December 1991
DMSP F11 SSM/I	01 January 1992	31 December 1995
DMSP F13 SSM/I	01 January 1996	31 December 2007
DMSP F17 SSMIS	01 January 2008	31 December 2016
DMSP F18 SSMIS	01 January 2017	31 December 2022
[1]Other data was not substituted for the missing SMMR data to cover the last 11 days of the melt season in August 1987. Those days are flagged as "no data."		

1.4.2 Resolution

Snow melt onset dates for each grid cell were derived once per year.

2 DATA ACQUISITION AND PROCESSING

2.1 Background

Accurate data for snow melt onset dates over sea ice contribute to improved simulations of climate during the Arctic snow melt period. Records of the spatial and temporal variability in snow melt can also serve as climate proxies in Arctic sea ice zones.

Snow melt onset dates are estimated based on changes in brightness temperature measurements. Microwave emissivity of snow increases dramatically as the snow melts and liquid water appears. With the presence of liquid water in the snow pack, surface scattering dominates over volume scattering, resulting in a sharp increase in the signature for brightness temperatures. Lower microwave frequencies (e.g. 18.0 GHz and 19.3 GHz) are more responsive to melt onset in ice than are higher frequencies (e.g. 37.0 GHz), primarily due to the change in emission depth associated with melt. Melt therefore causes the difference between low-frequency and high-frequency brightness temperatures to change from positive to near-zero or negative. Furthermore, the increase in brightness temperature associated with melt is polarization-dependent. Horizontal channels reflect a stronger dependence on snow conditions during melt due to the change in dielectric properties at the air-snow interface when snow is wet.

2.2 Acquisition

Snow melt onset dates were derived from brightness temperature (Tb) measurements and sea ice concentration (SIC) data acquired by the Scanning Multichannel Microwave Radiometer (SMMR), Special Sensor Microwave/Imager (SSM/I), and Special Sensor Microwave Imager/Sounder (SSMIS) instruments. Sea ice extent (SIE) masks, which were created based on SIC data, were used to constrain the melt algorithm. Table 8 describes the input data sources in more detail.

Table 8. Input Data Sets

Data Set	Description	Channels/ Variables Used
Nimbus-7 SMMR Polar Gridded Radiances and Sea Ice Concentrations, Version 1 (Gloersen 2006)	T_b used to calculate snow melt onset dates from 1979 to 1987.	18.0 GHz and 37.0 GHz
DMSP SSM/I-SSMIS Daily Polar Gridded Brightness Temperatures, Version 6 (Meier et al., 2021a)	T_b used to calculate snow melt onset dates from 1988 to 2022.	19.3 GHz and 37.0 GHz
NOAA/NSIDC Climate Data Record of Passive Microwave Sea Ice Concentration, Version 4 (Meier et al., 2021b)	Sea ice concentrations (SIC) used to a create mask of the maximum annual sea ice extent (SIE). Snow melt dates were only calculated for locations inside the sea ice mask.	cdr_seaice_conc

2.3 Processing

Snow melt onset dates were estimated using daily average brightness temperature (Tb) data from SMMR, SSM/I (F8, F11, and F13), and SSMIS (F17 and F18) satellite radiometers. Changes in 18.0 or 19.3 H-polarization GHz and 37.0 H-polarization GHz Tb were recorded for each grid cell using the Advanced Horizontal Range Algorithm (AHRA). For more details on AHRA, please refer to Drobot and Anderson (2001a).

The general steps for processing are as follows:

1. **Ensure consistent data input**
   For this data set, SSM/I F8 was used as the standard input sensor. Regression analysis was used on Tb measurements taken from SMMR, SSM/I F11 and F13, and SSMIS F17 and F18 and converted to Tb for SSM/I F8 (Abdalati et al., 1995; Stroeve et al., 1998; Meier et al., 2011; and Stewart et al., 2019, respectively). Note that because no additional inter-sensor calibration corrections were needed to correct Tb from F18 to the F8 baseline sensor (Stewart et al., 2019), Tb measurements for F17 and F18 used identical procedures and correction coefficients to correct to the baseline. Table 9 provides an overview of the correction coefficients used. Conversions were performed to ensure a consistent data record for determining temporal trends in the snow melt onset dates. If data are not

consistent, snow melt trends could be attributable to instrument characteristics rather than climate conditions.

2. **Create sea ice extent (SIE) mask**

   The *cdr_seaice_conc* variable of the NOAA/NSIDC Climate Data Record of Passive Microwave Sea Ice Concentration, Version 4 data set was used as a measure of daily Sea Ice Concentration (SIC). Based on a variable start date, these SIC estimates were used to determine maximum sea ice extent (SIE), that is, which pixels had a concentration of 50% or greater (SIC ≥ 50%).

3. **Run the AHRA algorithm**

   This current version of the AHRA algorithm has been updated to use a variable start date. The algorithm start date is now defined as the first day following the day of the annual maximum SIE. Snow melt onset dates (SMOD) were only calculated at pixel locations that met this criterion. The valid range of algorithm start dates now ranges from DOY 47 to DOY 91 with a mean of 66.2 (March 7th); and valid SMOD dates may range from DOY 40 to DOY 245.

   Once DOY was established, the AHRA calculates the difference between low-frequency (18.0 GHz or 19.3 GHz) and high-frequency (37.0 GHz) Tb measurements. When conditions are dry and frozen, low-frequency Tb measurements are larger than high-frequency Tb measurements. When low-frequency Tb drop below high-frequency Tb measurements, melt has started. Three major turn points are described below; for a more detailed discussion, refer to Drobot and Anderson (2001b).

   - If (18.0 / 19.3 GHz - 37.0 GHz) > 4 K, the AHRA assumes winter conditions and proceeds to the next day with data for that pixel.
   - If (18.0 / 19.3 GHz - 37.0 GHz) ≤ -10 K, the AHRA assumes liquid water was present in the snowpack and classifies that day as the snow melt onset date.
   - If 4 K > (18.0 / 19.3 GHz - 37.0 GHz) > -10 K, the AHRA determines if snow melt onset occurred based on a 20-day time series of Tb. The algorithm subtracts the minimum and maximum Tb values for the ten days prior to the potential melt onset date, and again for the period from the potential melt onset date to nine days later. The former number is then subtracted from the latter number. If the difference is greater than 7.5 K, the algorithm assigns a snow melt onset date to that particular grid cell because a large difference indicates variability in the 18.0 / 19.3 GHz - 37.0 GHz range after the potential melt onset date. If the difference was less than 7.5 K, then liquid water is unlikely to be in the snowpack, and the algorithm moves on to the next day.

4. **Assign quality flags for select pixels**

   Flag values were then assigned for select pixels, particularly when data represented open water; the pole hole; land mask; or no sea ice melt. See Table 1 for summary of flag values.

Table 9. Linear Regression Coefficients and Equations Used to Calibrate Tb Between SMMR, SSMI, and SSMIS Sensors using F8 as the Standard

Sensor Correction	Source	Overlap Area	Channels	Coefficients		Correction Equation
SMMR to F8	Jezek et al., (1991)	---	18H	Slope	0.940	F8 = (SMMR-2.62)/0.940
				Int. (K)	2.620	
			37H	Slope	0.954	F8 = (SMMR-2.85)/0.954
				Int. (K)	2.850	
F11 to F8	Abdalati et al., (1995)	Greenland	19H	Slope	1.013	F8 = 1.013*F11-1.890
				Int. (K)	-1.890	
			37H	Slope	1.024	F8 = 1.024*F11-4.220
				Int. (K)	-4.220	
F13 to F11	Stroeve et al., (1998)	NH Sea Ice	19H	Slope	0.986	F11 = (F13-2.197)/0.986
				Int. (K)	2.179	
			37H	Slope	0.966	F11 = (F13-6.110)/0.966
				Int. (K)	6.11	
F17 to F13	Meier et al., (2011)	Arctic Mar - Sept 2007	19H	Slope	0.979	F13 = (F17-1.646)/0.979
				Int. (K)	1.646	
			37H	Slope	0.999	F13 = (F17-0.649)/0.999
				Int. (K)	0.649	
F18 to F13	Stewart et al., (2019)	Arctic Mar - Sept 2007	19H	Slope	0.979	F18 = (F18-1.646)/0.979
				Int. (K)	1.646	
			37H	Slope	0.999	F18 = (F18-0.649)/0.999
				Int. (K)	0.649	

2.4 Quality, Errors, and Limitations

2.4.1 Differences between V5 and previous versions

The algorithm (i.e., melt season) start date is now variable. Unlike previous versions, where for the AHRA algorithm had a fixed Day of Year (DOY) as 61 (March 2nd, or March 1st in leap years), this updated version has a variable start date. The algorithm start date is now defined as the first day following the day of the annual maximum sea ice extent (SIE), with valid start dates now ranging from DOY 47 to DOY 91 with a mean of 66.2 (March 7th); and valid SMOD dates ranging from DOY 40 to DOY 245. Updating the AHRA algorithm start date has two major advantages. First, the first possible melt onset date is the day after the sea ice reaches its maximum extent. Second, the earliest melt onset dates now better correspond with the seasonal shift to the melt season as well as subsequent sea ice retreat for that particular year.

2.4.2 Error Sources

Brightness temperature data may have errors related to pixel averaging, sensor errors, and weather effects. See the following brightness temperature documentation for more information regarding errors in the source data:

- DMSP SSM/I-SSMIS Daily Polar Gridded Brightness Temperatures
- Nimbus-7 SMMR Polar Radiances and Arctic and Antarctic Sea Ice Concentrations

2.4.3 Limitations

Given the known errors, users are advised against selecting individual pixels without examining surrounding data points. Also, trend analysis at any given pixel should include a study of nearby pixels to confirm that results are locally consistent.

2.5 Instrumentation

Brightness temperature input data were acquired from the Scanning Multichannel Microwave Radiometer (SMMR), Special Sensor Microwave/Imager (SSM/I), and Special Sensor Microwave Imager/Sounder (SSMIS) instruments. For more details, refer to the SMMR, SSM/I, and SSMIS Sensors Summary.

3 SOFTWARE AND TOOLS

For a comprehensive list of all polar stereographic tools, see the Does NSIDC have Tools to Extract and Geolocate Polar Stereographic Data? Web page.

4 VERSION HISTORY

Table 10 outlines the processing and algorithm history for this product.

Table 10. Description of Version Changes

Version	Date	Description of Changes from Previous Version
V05	Dec 2022	Extended the data record through 2021; and reprocessed the entire data set using a newer version of the sea ice extent masks within the snow melt onset algorithm. The Advanced Horizontal Range Algorithm (AHRA) has been updated to have a variable start date. The algorithm start date is now defined as the first day following the day of the annual maximum sea ice extent (SIE), making the first possible melt onset date as the day after the sea ice reaches its maximum extent. To derive the sea ice mask and identify maximum annual SIE, the *cdr_seaice_conc* variable was used as daily sea ice concentrations.
V04	June 2019	Reprocessed the entire data set using a newer version of the sea ice extent masks within the snow melt onset algorithm. No other changes were made to the algorithm. Extended the data record through 2017. After snow melt dates were computed, flags were added to the data to indicate where snow melt dates were not derived. The flags discriminate between sea ice where the snow melt onset date was not found and pixels included in the land mask, the pole hole, and areas of open water. Updated data fields that summarize basic statistics over the length of the data record. Data are now distributed as a netCDF file.
V03	Mar 2014	Extended data record through the 2012 melt season which includes the use of the SSMIS instrument on the DMSP F17 satellite. Removed the two-pixel buffer surrounding the coastlines. Included the use of an annual sea ice extent mask to indicate sea ice locations where a melt onset date was calculated. Changed the regression coefficients used to convert the F11 brightness temperatures to ones from Stroeve et al. (1998). Changed parameter values from 0 to 255 (inclusive) to 0 to 245 (inclusive). Trend files are no longer being generated. Used the gsfc_25n.msk land/coast mask.
V02	Nov 2009	Removed 9-point median filter that corrected for spurious melt dates in V01 Added flags to input brightness temperatures to correct for bad scanlines, then reprocessed input brightness temperatures.

Version	Date	Description of Changes from Previous Version
V01	Dec 2001	Original version of data.

5 RELATED DATA SETS

- MEaSUREs Arctic Sea Ice Characterization Daily 25km EASE-Grid 2.0 (NSIDC-0532)
- DMSP SSM/I-SSMIS Daily Polar Gridded Brightness Temperatures (NSIDC-0001)
- Nimbus-7 SMMR Polar Radiances and Arctic and Antarctic Sea Ice Concentrations (NSIDC-0007)
- Sea Ice Concentrations from Nimbus-7 SMMR and DMSP SSM/I-SSMIS Passive Microwave Data (NSIDC-0051)
- Bootstrap Sea Ice Concentrations from Nimbus-7 SMMR and DMSP SSM/I-SSMIS (NSIDC-0079)
- NOAA/NSIDC Climate Data Record of Passive Microwave Sea Ice Concentration

6 RELATED WEBSITES

- SMMR, SSM/I, and SSMIS Sensors Summary
- Polar Stereographic Projection and Grid
- Does NSIDC have Tools to Extract and Geolocate Polar Stereographic Data?

7 REFERENCES

Abdalati, W., K. Steffen, C. Otto and K. Jezek. 1995. Comparison of brightness temperatures from SSM/I Instruments on the DMSP F8 and F11 Satellites for Antarctica and the Greenland Ice Sheet. *International Journal of Remote Sensing* 16:1223-1229. DOI: https://doi.org/10.1080/01431169508954473.

Anderson, M. 1997. Determination of a Melt Onset Date for Arctic Sea Ice Regions Using Passive Microwave Data. *Annals of Glaciology* 25:382-387. DOI: https://doi.org/10.3189/s0260305500014324.

Drobot, S. D., and Anderson, M. R. 2001a, An improved method for determining snowmelt onset dates over Arctic sea ice using scanning multichannel microwave radiometer and Special Sensor Microwave/Imager data, J. Geophys. Res., 106(D20), 24033-24049. DOI: https://doi.org/10.1029/2000JD000171.

Drobot, S. and M. Anderson. 2001b. Comparison of Interannual Snowmelt Onset Dates with Atmospheric Conditions. *Annals of Glaciology* 33: 79-84.
DOI: https://doi.org/10.3189/172756401781818851.

Gloersen, P. 2006. *Nimbus-7 SMMR Polar Gridded Radiances and Sea Ice Concentrations, Version 1.* [1979-1987]. Boulder, Colorado USA. NASA National Snow and Ice Data Center Distributed Active Archive Center. DOI: https://doi.org/10.5067/QOZIVYV3V9JP.

Jezek, K., C. Merry, D. Cavalieri, S., Grace, J. Bedner, D. Wilson, and D. Lampkin. 1991. Comparison Between SMMR and SSM/I Passive Microwave Data Collected over the Antarctic Ice Sheet. Byrd Polar Research Center Technical Report No. 91-03, The Ohio State University, Columbus, Ohio, 62 pp. (See PDF)

Meier, W. N., Khalsa, S. J. S., and M. H. Savoie. 2011. Intersensor calibration between F-13 SSM/I and F-17 SSMIs near-real-time sea ice estimates. *IEEE Trans. Geosci. Remote Sens.* 49:3343–3349. DOI: https://doi.org/10.1109/TGRS.2011.2117433.

Meier, W. N., J. S. Stewart, H. Wilcox, D. J. Scott, and M. A. Hardman. 2021a. *DMSP SSM/I-SSMIS Daily Polar Gridded Brightness Temperatures, Version 6*. [1988-2021]. Boulder, Colorado USA. NASA National Snow and Ice Data Center Distributed Active Archive Center. DOI: https://doi.org/10.5067/MXJL42WSXTS1.

Meier, W. N., F. Fetterer, A. K. Windnagel, and J. S. Stewart. 2021b. *NOAA/NSIDC Climate Data Record of Passive Microwave Sea Ice Concentration, Version 4*. [1979-2021]. Boulder, Colorado USA. NSIDC: National Snow and Ice Data Center. DOI: https://doi.org/10.7265/efmz-2t65.

Stewart, S., H. Wilcox, W. Meier, and D. Scott. 2019. Comparison of F17 and F18 Daily Polar Gridded SSMIS Data. National Snow and Ice Data Center, Boulder: CO. (See PDF)

Stroeve, J., J. Maslanik, and L. Xiaoming. 1998. An Intercomparison of DMSP F11- and F13-derived Sea Ice Products. *Remote Sensing of the Environment 64:132-152.* DOI: https://doi.org/10.1016/S0034-4257(97)00174-0.

8 DOCUMENT INFORMATION

8.1 Publication Date

December 2022

8.2 Date Last Updated

August 2023